Title

Kilohertz Transcranial Magnetic Perturbation (kTMP): A New Non-invasive Method to Modulate Cortical Excitability

Author names and affiliations

Ludovica Labruna*[1,2,3], Christina Merrick*[1,2], Angel V Peterchev[4,5,6,7], Ben Inglis[3], Richard B Ivry[1-3], Daniel Sheltraw[1,3]

*co–first authors.

[1]Magnetic Tides, Inc., El Cerrito, CA 94530, USA

[2]Department of Psychology, University of California, Berkeley, CA 94704, USA

[3]Helen Wills Neuroscience Institute, University of California, Berkeley, CA 94704, USA

[4]Department of Psychiatry and Behavioral Sciences, Duke University, Durham, NC 27710, USA

[5]Department of Biomedical Engineering, Duke University, Durham, NC 27708, USA

[6]Department of Electrical and Computer Engineering, Duke University, Durham, NC 27708, USA

[7]Department of Neurosurgery, Duke University, Durham, NC 27710, USA

Corresponding author: Ludovica Labruna, Magnetic Tides Inc., email: lulabrun@gmail.com.

Abstract

Background: Non-invasive brain stimulation (NIBS) provides a method for safely perturbing brain activity, and has been employed in basic research to test hypotheses concerning brain-behavior relationships with increasing translational applications.

Objective: We introduce and evaluate a novel subthreshold NIBS method: kilohertz transcranial magnetic perturbation (kTMP). KTMP is a magnetic induction method that delivers continuous kHz-frequency cortical electric fields which may be amplitude-modulated to potentially mimic electrical activity at endogenous frequencies.

Methods: We used TMS to compare the amplitude of motor-evoked potentials (MEPs) in a hand muscle before and after kTMP. In Experiment 1, we applied kTMP for 10 min over motor cortex to induce an E-field amplitude of approximately 2.0 V/m, comparing the effects of waveforms at frequencies of 2.0, 3.5, or 5.0 kHz. In Experiments 2 and 3 we used two forms of amplitude-modulated kTMP with a carrier frequency at 3.5 kHz and modulation frequencies of either 20 or 140 Hz.

Results: The only percept associated with kTMP was an auditory tone, making kTMP amenable for double-blind experimentation. Relative to sham stimulation, non-modulated kTMP at 2.0 and 3.5 kHz resulted in an increase in cortical excitability, with Experiments 2 and 3 providing a replication of this effect for the 3.5 kHz condition. Although amplitude-modulated kTMP increased MEP amplitude compared to sham, no enhancement was found compared to non-modulated kTMP.

Conclusions: kTMP opens a new experimental NIBS space inducing relatively large amplitude subthreshold E-fields able to increase cortical excitability with minimal sensation.

Keywords: non-invasive brain stimulation, high frequency magnetic induction, electric field, amplitude modulation, transcranial magnetic stimulation, subthreshold.

Introduction

Electromagnetic non-invasive brain stimulation (NIBS) refers to a group of methods which perturb brain function by coupling an applied electric field (E-field) to neurons without the need to introduce electrodes into brain tissue. The NIBS E-field can safely manipulate neural excitability, providing neuroscientists with a powerful tool to advance our understanding of brain function. Evidence that NIBS can promote brain plasticity [1] has prompted clinicians to pursue NIBS interventions in the treatment of psychiatric and neurologic disorders [2–7].

The NIBS E-field amplitude can be categorized as subthreshold or suprathreshold. Suprathreshold fields are sufficient to elicit immediate action potentials in neurons initially at resting membrane potential. Subthreshold E-fields are insufficient to directly cause action potentials but are employed to alter the state of the targeted neurons on time scales ranging from immediate entrainment effects to plasticity effects that extend well past the stimulation epoch [8,9]. As such, subthreshold and suprathreshold methods have different experimental and clinical utilities.

Two broad categories of NIBS methods exist, delivering the E-field to the brain via injection of current through electrodes contacting the scalp or magnetic induction from a coil placed over the scalp. In electrical methods, such as transcranial electrical stimulation (tES), the current and E-field can be constant as in transcranial direct current stimulation (tDCS) or time varying as in transcranial alternating current stimulation (tACS). Magnetic

induction methods, such as transcranial magnetic stimulation (TMS), deliver a time-varying current to the coil, generating a changing magnetic field and consequently an induced E-field in superficial brain regions. TMS is delivered as a brief pulse (typically 200–300 μs) and is referred to as repetitive TMS (rTMS) when delivered as a train of pulses.

The E-fields of tES and TMS differ in important ways [10]. First, for TMS the E-field amplitude is linearly proportional to the frequency of the current source, whereas the tES E-field amplitude is independent of this frequency. Second, the E-fields for the two methods exist in orthogonal subspaces. While they can never be spatially identical, they can in principle be spatially similar with respect to focality on the cortical surface.

Third, for spatially similar cortical E-fields, the scalp E-field amplitude for tES is much greater than the scalp E-field for TMS and the ratio of these amplitudes increases with cortical focality [10,11]. Thus, the scalp E-field amplitude ultimately places a severe constraint on the focality and amplitude of tES cortical E-fields due to scalp peripheral nerve stimulation and muscle stimulation. Estimates of the tES cortical E-fields in the physiological frequency range suggest that the maximum for most human participants is around 0.5 V/m [12,13]; beyond this value scalp stimulation becomes detectable and soon intolerable. TMS systems are far less burdened by constraints imposed by the scalp E-field amplitude, allowing the method to be used to produce both subthreshold and suprathreshold cortical E-fields.

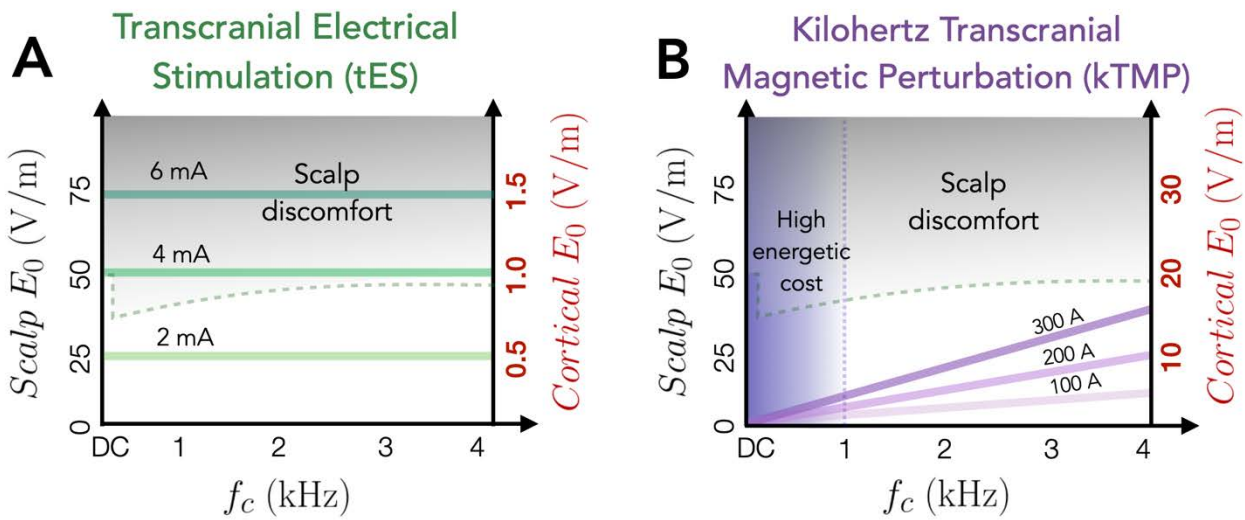

Figure 1. An illustration of the practical constraints of tES and kTMP in frequency and amplitude space. Solid lines represent the dependency of the electric field amplitude upon frequency and amplitude of the electric current supplied to the electrodes (A) or coil (B). Calculations are based on for a typical 5 × 7 cm tES electrode montage or figure-of-eight TMS/kTMP coil. Left vertical axis represents estimated scalp E-field amplitude while the right vertical axis represents the estimated motor cortex E-field amplitude. Shaded zones represent regions of the perturbation space constrained by practical considerations. Both methods are constrained by the scalp E-field magnitude, which at high values may result in discomfort due to peripheral nerve stimulation (gray shading). The gray dashed function depicts the dependence of scalp stimulation threshold upon frequency [14]. Note the substantial difference in the cortical E-field range that can be delivered tolerably for tES and kTMP. Illustrated here are approximate levels of discomfort for sustained waveforms (tES and kTMP) as opposed to pulsed methods (e.g., TMS). Note that magnetic induction methods such as kTMP (or TMS) are additionally constrained by high energetic costs (purple shading) required to generate E-fields of sufficient magnitude to influence neuronal states at low frequencies.

Motivated by these considerations, we developed a new magnetic induction NIBS approach, in which the subthreshold modulation of neural excitability is brought about via oscillating magnetic fields at kHz frequencies. We refer to this system as kTMP (kilohertz Transcranial Magnetic Perturbation). In our new method, we drive a TMS coil using a high-current large-bandwidth amplifier operating in the kHz range. In this way, the E-field magnitude constraints imposed by scalp stimulation associated with tES are greatly diminished (Fig 1). The energetic requirements for magnetic induction system would be prohibitive at low frequencies such as those measured with EEG. However, this cost is reduced to a manageable level by operating at higher frequencies. While the prototype

kTMP system used in the present experiment produced cortical E-fields of 2 V/m at 2 – 5 kHz, kTMP has the potential to significantly increase the range of subthreshold E-field induction with the focality typical of TMS systems. In addition, the kTMP waveform can be amplitude modulated to potentially mimic E-fields at frequencies matching endogenous neural rhythms [15].

Since neurons near resting membrane potential act as low-pass filters, a critical question centers on whether narrow band kHz E-fields can effectively couple to the transmembrane potential to influence neural activity. This question has been explored in invasive and non-invasive empirical studies (reviewed in [16]) and in model simulations [17]. Experimentally, suprathreshold kHz fields have been used to produce nerve blocking [18] and temporal interference effects [19]. Converging evidence also indicates that subthreshold kHz fields are effective in modulating neural excitability. In particular, kHz tACS can induce increases in post-stimulation motor-evoked potentials approximately equal to that observed following standard, low frequency tES or rTMS [20,21]. Intriguingly, low frequency magnetic stimulation (LFMS), a kHz method that mimics the magnetic field waveforms used in MRI, applies weak kHz E-fields across most of the brain and has been reported to have mood-altering effects [22–26]. In addition, kHz E-fields, again applied by MRI gradients, have been shown to alter brain glucose metabolism in a manner that scales with the field amplitude [27].

We report here the results of three experiments with healthy human participants that evaluate the efficacy of kTMP in modulating cortical excitability. Adopting a conventional approach for evaluating the efficacy of NIBS methods [28–31], we used suprathreshold TMS to measure motor evoked potentials (MEPs) elicited in a hand muscle, comparing the amplitude of the MEPs before and after kTMP stimulation. For all the experiments, the kTMP amplitude was set to a produce a peak cortical E-field amplitude of approximately 2.0 V/m at the targeted primary motor cortex. In Experiment 1, we tested non-amplitude modulated kTMP at three different carrier frequencies (2 kHz, 3.5 kHz and 5 kHz), comparing these conditions to a sham condition (0.01 V/m at 3.5 kHz). In Experiment 2 and 3, the carrier frequency was fixed at 3.5 kHz and we investigated two forms of amplitude-modulated kTMP (AM kTMP) with modulation frequencies of either 20 Hz or 140 Hz.

Methods

Apparatus

The **kilohertz transcranial magnetic perturbation (kTMP)** system consists of a high-amplitude current source, a TMS coil, and a control system. The same TMS coil may be connected to either the kTMP current source or to a commercial TMS pulse generator (MagVenture MagPro R30 with MagOption), permitting interleaved kTMP-TMS experiments and ensuring identical kTMP and TMS E-field distributions up to an amplitude scaling factor. The kTMP amplifier (AE Techron Model 7794) is a voltage-controlled current source capable of delivering up to 200 A to the coil. We used an actively-liquid-cooled figure-of-eight coil (MagVenture Cool-B65; inner and outer loop diameter of 35 mm and 75 mm, respectively).

The kTMP control system consists of a personal computer (PC), input/output PCI card, and a custom interface to read the coil's built-in temperature sensor. Using a data acquisition toolbox (Mathworks R2018a), the PCI card was programmed to deliver analog input to the amplifier, thus specifying the temporal waveform of the E-field. The input waveform can either be at a fixed-amplitude sinusoidal frequency (non-modulated) or amplitude modulated.

Bench testing indicated that the system when running in kTMP mode did not produce marked changes in coil temperature. As an added safeguard, the PCI card was set up to receive an analog input from the coil's temperature sensor and create an automatic shutdown if the coil temperature exceeded 41° C, which is within the guidelines established by the International Electrotechnical Commission (IEC). In practice, for E-fields up to 2 V/m used in the present experiments, the coil temperature never rose above 32° C during system operation.

Participants

Forty-nine young adults were recruited through various advertisements posted to the Berkeley community. The number of participants in Experiments 1, 2, and 3 was 16 (12 female), 16 (10 female), and 15 (11 female), respectively. Seven of the participants in Exp 2 had also been tested in Exp 1 (minimum 3 weeks between the last session of Exp 1 and first session of Exp 2). All participants were naive to the purpose of the study, provided informed consent, and were financially compensated. Given the novelty of kTMP

as a NIBS method, the IRB at UC Berkeley enlisted an outside expert and members of the campus Environmental and Health Safety Committee to evaluate the system. Following their reports, the protocol was approved by the IRB at UC Berkeley with the kTMP system deemed a non-significant risk device for E-fields up to 8 V/m for up to 20 min of stimulation.

Procedure

To evaluate the kTMP system as a new tool to modulate neuronal excitability, we measured the impact of kTMP on corticospinal excitability using suprathreshold TMS stimulation over motor cortex. Figure 2 depicts an overview of the experimental hardware and protocol. In brief, kTMP stimulation was preceded by two 4–7 min probe blocks and followed by three such blocks. For Exps 1 and 2 each block consisted of a trio of TMS assays of cortical excitability; for Exp 3 only single-pulse TMS was assessed (described further below).

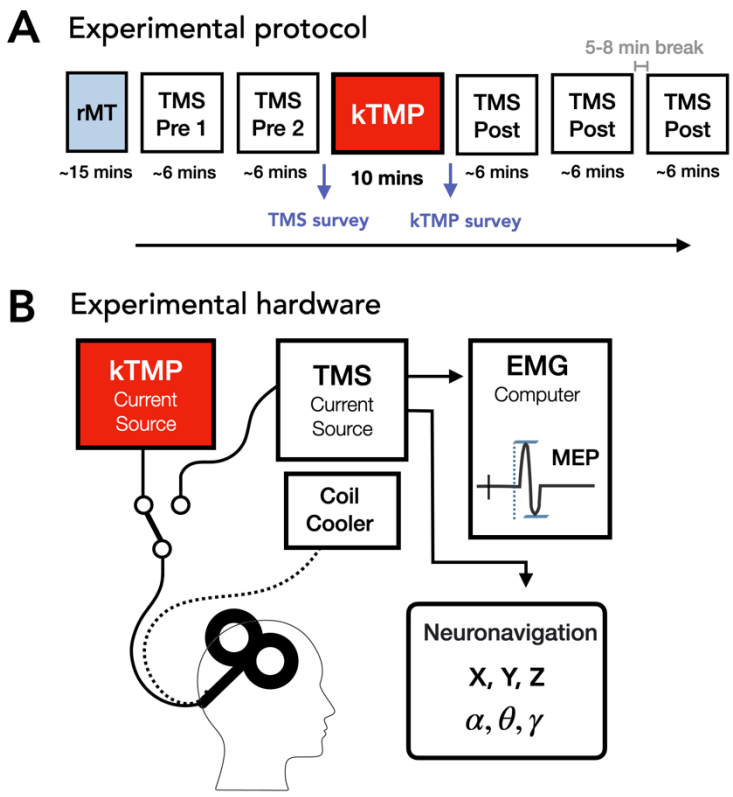

Figure 2. Experimental protocol and hardware. A. Timing of each experimental session. After determining the participant's resting motor threshold (rMT), TMS assessment blocks were conducted before (Pre) and after (Post) kTMP stimulation (active or sham). **B.** The same coil was driven by either the TMS current source or the kTMP current source. TMS pulses were recorded in an auxiliary channel of the EMG and triggered the neuronavigation system to record the coordinates of the coil in 3-D space.

Each experiment consisted of five 2-hr test sessions, with each session separated by a minimum of 2 days. The first test session was used to determine the optimal coil position ("hotspot") and threshold intensity for eliciting MEPs with suprathreshold single-pulse TMS (see below). The position of the hotspot was recorded by a neuronavigation system (Brainsight, Rogue Research, Montreal, Canada). This allowed the experimenter to return to the same position for each TMS block (see below), as well as during the application of kTMP. The other four sessions were used to test the efficacy of different kTMP parame-

ters on cortical excitability, with a focus on variation of the carrier frequency for non-modulated kTMP in Exp 1 and both non-modulated and amplitude-modulated kTMP in Exp 2 and Exp 3.

Two steps were taken to create a double-blinding protocol. First, we created a coding system such that the experimenter typed in a number that was paired to the desired stimulation condition in an arbitrary and random manner, one that varied across participants in a manner unknown to the experimenter. Second, we played a tone at 3.5 kHz using the Tone Generator Application Sonic™ (VonBruno 2015) to create a constant background sound during kTMP stimulation in all conditions, including sham, effectively masking the amplifier sound.

kTMP

For each carrier frequency, the current amplitude was selected to achieve a peak E-field amplitude of 2.0 V/m at a distance of 14 mm perpendicular to the coil surface, a distance we took to represent the approximate depth of the motor cortex from the overlying scalp [32]. A triangular loop probe [33] was used to measure the effective E-field amplitude in a spherical conductor approximating the human head. The relationship between the current amplitude I (units of A), carrier frequency f_c (units of Hz), and cortical E-field amplitude E_0 (units of V/m) was established to be:

$$E_0 = k f_c I$$

$$k = 7.875 \times 10^{-6} \frac{\mathrm{Vs}}{\mathrm{Am}}$$

where V, s, A, and m, correspond to volts, seconds, amperes, and meters, respectively.

Experiment 1. Non-modulated kTMP

We used a within-subject design, testing each participant on each of four kTMP stimulation conditions, with the order counter-balanced across participants. For three of the conditions, the carrier frequency (2 kHz, 3.5 kHz, 5 kHz) was paired with an intensity to create an E-field at the superficial aspect of the hand area of the motor cortex of $E_0 = 2$ V/m. We set the non-modulated E-field to be a sinewave with frequency f_c (see Fig 2):

$$E_{NM}(t) = E_o \cos(2\pi f_c t)$$

Note that we did not adjust for individual differences in scalp-to-cortex distance. For the sham condition, we used a 3.5 kHz carrier frequency producing a 0.01 V/m E-field at the approximate distance of the cortical surface.

Experiments 2 and 3. Amplitude-modulated kTMP (AM kTMP)

For Exps 2 and 3 we again used a within-subject design, testing each participant in four sessions. Two of the conditions were repeated from Exp 1: the 3.5 kHz non-modulated kTMP at 2 V/m and the sham condition. For the other two conditions, the carrier frequency was set at 3.5 kHz and the waveform was amplitude modulated (AM) at modulation frequencies of either 20 Hz or 140 Hz. The 3.5 kHz carrier frequency was chosen since we had obtained the largest effect size compared to sham at this frequency in Exp 1. We selected the 20 Hz modulation frequency given the relevance of beta to motor function [34–36] and the 140 Hz modulation frequency based on literature concerning ripple effects at this frequency [37–39]. The peak cortical E-field amplitude for the AM conditions

was 2 V/m, identical to the non-modulated condition. Note that the inclusion of the 3.5 kHz non-modulated condition and sham for both experiments provides two replications of these conditions from Exp 1 as well as points of comparison for the AM kTMP conditions.

Exps 2 and 3 differed in the form used for amplitude modulation. In general, an amplitude modulated current can be written as

$$E(t) = A(t)\sin(2\pi f_c t).$$

where $A(t)$ is a time dependent amplitude modulation factor. A popular form used in communications systems is:

$$A(t) = E_o[a + mf(t)]$$

where $f(t)$ is the signal one wishes to convey between two components of a system and the ratio m/a is the modulation index. The modulation index is typically chosen to suit the proposed means of demodulation.

In *Experiment 2,* we used $f(t) = \sin(2\pi f_m t)$ and an infinite modulation index. Correspondingly the E-field has time dependence of the form:

$$E_{AM1}(t) = E_o \sin(2\pi f_m t)\sin(2\pi f_c t)$$

where f_m is the modulation frequency. In Experiment 3, we used $f(t) = \sin(2\pi f_m t)$ and a modulation index of one (see Fig 3).

$$E_{AM2}(t) = E_o\left[\frac{1}{2} + \frac{1}{2}\sin(2\pi f_m t)\right]\sin(2\pi f_c t).$$

Although the same modulation frequencies are used to calculate E_{AM1} and E_{AM2} they differ with respect to the spectrum of their upper envelope, the frequency of which we refer to as the burst repetition frequency (f_b). For E_{AM1} the burst repetition frequency is double that of the modulation frequency, whereas for E_{AM2} the burst repetition frequency and the modulation frequency are matched. The burst repetition frequency may be an important parameter in determining the neural effects of kTMP.

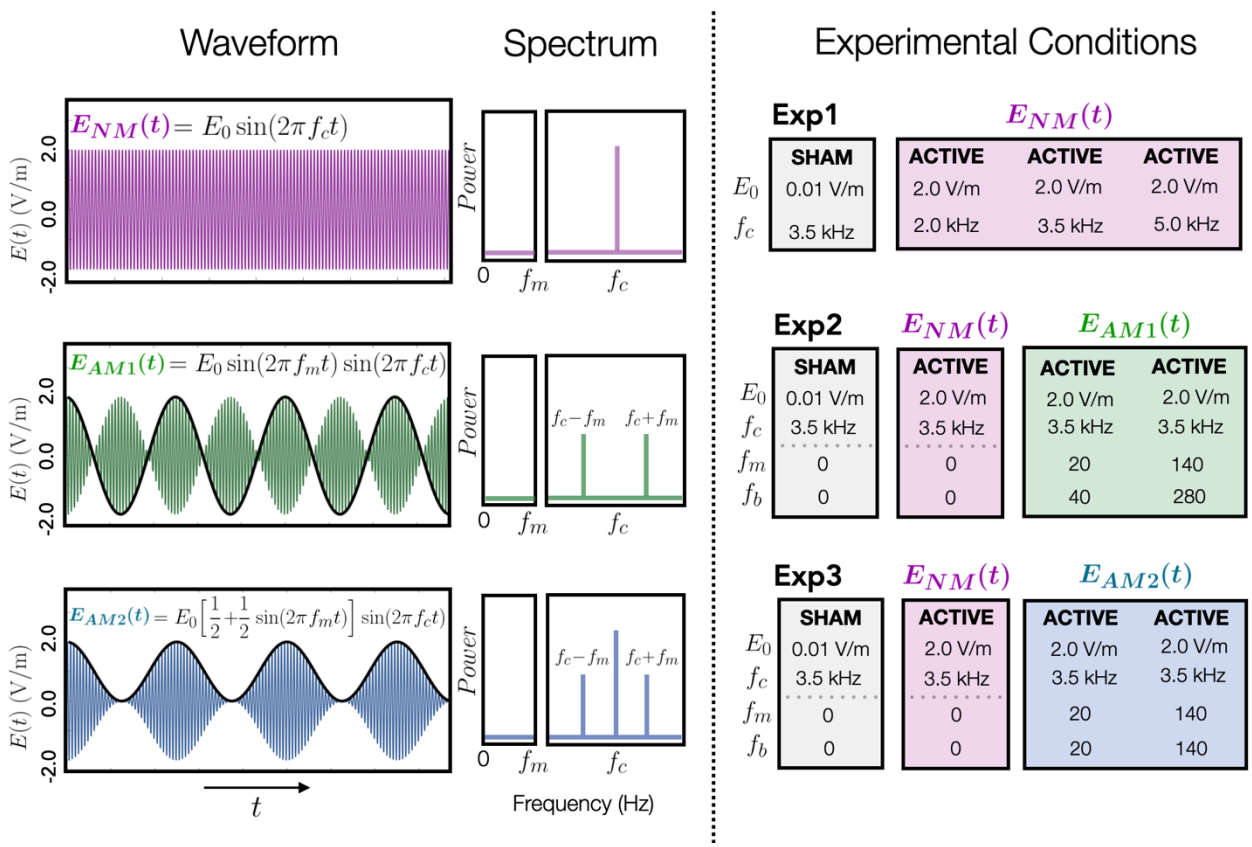

Figure 3. Waveforms, spectra and conditions for the three kTMP experiments. A commonly used form of amplitude modulation is $E(t) = E_0[a + m\sin(2\pi f_m t)]\sin(2\pi f_c t)$. The constants f_c, f_m, and E_0 refer to the carrier frequency, modulation frequency and the E-field amplitude (cortical E-field) respectively. Left column, Waveforms: E_{NM}, E_{AM1} and E_{AM2} refer to the non-modulated waveform and the two forms of amplitude modulation tested. Black lines indicate the modulation frequency. Center column, Spectrum: Carrier frequency and sidebands for the corresponding waveforms. Note the absence of power at the modulated frequency (f_m). Right column, Waveform parameters and characteristics for each experiment. f_b refers to the burst repetition frequency.

TMS: Hotspot and Threshold Procedure (Session 1)

Single-pulse TMS was applied over left hemisphere primary motor cortex to determine the resting motor threshold (rMT) for the first dorsal interosseous muscle (FDI) in the right hand. We focused on FDI since it is relatively easy to isolate in all individuals and threshold values are stable across test sessions [e.g., 40–42].

The TMS coil was placed tangentially on the scalp with the handle pointing backward and laterally at 45° from the midline. TMS was administered with a biphasic pulse waveform with a posterior–anterior direction of the second, dominant phase of the induced current. The stimulator intensity was initially set to 30% of maximal stimulator output and single pulses were generated at 5 s intervals, with the experimenter visually monitoring the electromyography (EMG) output for MEPs. If no MEPs were detected after 2 or 3 pulses, the experimenter moved the coil a few mm. If a search over the candidate area failed to produce any MEPs, the stimulator output was increased (step size of 3%), with the location search repeated. Once MEPs were detected, a more focal search was conducted to identify the optimal location for eliciting MEPs. This location was registered in three-dimensional space relative to the subject's head using the Brainsight neuronavigation system to ensure consistent coil position during and between experimental sessions. rMT was defined as the minimum TMS intensity required to evoke MEPs of at least 50 µV peak-to-peak amplitude on 5 of 10 consecutive trials.

The mean threshold was 58% (SD = 11.3%), 63% (SD = 11.1%) and 56% (SD = 9.2%) of maximum stimulator output in Experiments 1, 2 and 3 respectively. We repeated the

threshold procedure in each of the kTMP sessions to capture possible intra-individual baseline changes in the cortico-excitability of the participants. In practice, the individual's threshold values remained very stable across days (SD = 2.4%).

TMS Assays of Corticospinal Excitability (Sessions 2-5)

For Exps 1 and 2, each of the five probe blocks (two pre-kTMP and three post-kTMP) included single-pulse TMS (SP), and two paired-pulse protocols: short intracortical inhibition (SICI) and intracortical facilitation (ICF) [43,44]. Similar to SP, paired pulse protocols were administered with biphasic pulse waveforms with a posterior–anterior direction of the second, dominant phase of the induced current. These three protocols have been widely used in prior studies designed to evaluate the efficacy of tES and rTMS methods in altering neural excitability [45–47]. For SP, the stimulation level was set at 120% of rMT. For the paired-pulse assays, the suprathreshold pulse was preceded by a subthreshold conditioning stimulus set at 80% of rMT, with an interstimulus interval (ISI) of 3 ms or 10 ms for SICI and ICF, respectively. The probe block consisted of 90 trials, 30 for each of the three assays, with the order randomized within the block. For Exp 3, the five probe blocks consisted only of the single-pulse TMS assay. We made this decision after finding that kTMP had no effect on SICI or ICF in Exps 1 and 2. We lengthened the breaks between blocks in Exp 3 to match the timing of the three post blocks relative to kTMP stimulation in the first two experiments.

We developed a system to read and record the spatial and angular position of the coil with respect to the hotspot in real time from Brainsight. This information was recorded at

the time of each TMS pulse and used to exclude trials in which the coil was distant from the hotspot or the angle had changed from the optimal hotspot orientation.

EMG

EMG activity was recorded (Bagnoli-8 EMG System, Delsys Inc.) from surface electrodes placed over the right FDI muscles, with a reference electrode over the right elbow. The experimenter visually inspected the EMG traces on a monitor to ensure that the participant remained relaxed (i.e., negligible EMG background activity in FDI), to detect the presence or absence of MEPs in response to the TMS pulses, and, since kTMP is a novel brain stimulation modality, to monitor for safety by checking for after discharges or other features suggesting excessive increase in excitability that could evolve into a seizure.

The EMG signal was amplified and bandpass filtered on-line between 20 and 450 Hz. The signals were digitized at 2000 Hz for offline analysis. All EMG measures were analyzed with custom scripts written in Matlab 2018a. EMG was recorded continuously during the experiment. Offline, data were segmented based on a TTL pulse from the TMS system recorded by the EMG amplifier on an auxiliary channel.

Subjective Reports

We informally assessed the participants' subjective experience in Exp 1, focusing on reports concerning the perception of sound emitted from the system, tactile sensation, and discomfort. This process was formalized in Exps 2 and 3. In these studies, we adminis-

tered a short survey in which participants answered three questions concerning 1) annoyance, 2) pain, and 3) subjective experience of muscle activation/movement. Participants responded to each question using a keyboard to type in a number using an 11-point scale (0 = not at all; 10 = extremely). This survey was based on a systematic rating system that has been employed to characterize the degree of disturbance caused by TMS [48]. We administered the survey twice. The first time was after the second TMS probe block, providing ratings on the subjective experience of suprathreshold TMS. The second time was after kTMP, providing ratings on the subjective experience of kTMP stimulation.

Data analysis

MEP Data

For each trial, the peak-to-peak amplitude of the MEP was calculated over a window 15–45 ms after the suprathreshold TMS pulse. Trials were excluded from the analysis based on the following criteria: 1) If the MEP amplitude was 2.5 standard deviations above or below the mean, with the mean and standard deviation calculated separately for each TMS assay (SP, ICF, SICI) for each probe block. 2) If the Brainsight recording indicated that the coil was more than 3 mm (Euclidian distance) from the optimal hotspot location or had an angular or twist error more than 5º from the optimal trajectory angle. 3) If noise in the EMG signal 100 ms before the TMS pulse exceeded 2.5 standard deviations of the mean EMG signal. On average 10% (SD = 3%) of the trials were excluded per participant with a range of 4.8% to 20%. After cleaning the MEP data, there were a minimum of 20 MEP measures per protocol in each assessment block for each individual, a sufficient number for performing the MEP analyses [46,49–51].

Raw MEP amplitudes were log-transformed to normalize the distribution of MEP amplitudes [52–55]. The average log-transformed MEP amplitude was then calculated for each of the three TMS protocols in each probe block on an individual basis. After averages were calculated, the data were exponentiated to get the MEPs back to an easily interpreted scale (i.e., mV). SICI and ICF measures were calculated by computing a ratio of the paired-pulse MEP average over the single pulse MEP average for each block. For all three TMS assays the effect of kTMP stimulation was operationalized as the average percent change post kTMP relative to the two baseline blocks (averaged). For example, a value of 0% would indicate no change in single-pulse MEP amplitude from pre- to post-stimulation, whereas a value of 100% would indicate the single-pulse MEP amplitude doubled from pre- to post-stimulation. Thus, the main analysis focuses on the three post-kTMP stimulation probe blocks for each of the three TMS assays (SP, SICI, ICF).

Missing data

Although we aimed for a fully within-subject design, a subset of the participants only had data for three of the four sessions. Missing data were due to 1) technical issues with the Brainsight neuronavigation system (n = 2/47), 2) university suspension of testing with human participants in March 2020 due to the onset of the COVID-19 pandemic (n = 5/47), or 3) determination that the results from a session were a statistical outlier (n = 3/47). The latter three had an increase in corticospinal excitability three standard deviations above the mean in one condition. All of these were active kTMP conditions and, if included would have inflated the effect of kTMP on corticospinal excitability. To account for missing data

and subject variability, all analyses used a linear mixed-effects model with a random factor of participant.

Linear mixed effects models

Linear mixed effects models were implemented in RStudio using the software package lme4 [56]. Each mixed effects model used participant as a random effect and experimental variables (e.g., active vs. sham, post-stimulation block) as fixed effects. For the null model, participant was treated as a random effect to predict average MEP values, and nested models were created to evaluate each of the fixed effects. The fixed factors were added to the model to assess if a factor significantly improved prediction above that obtained with the null model. Interactions were tested by comparing a model in which the fixed effects were restricted to be additive against a second model that could have multiplicative and additive effects. Cohen's *d* was calculated based on the methods outlined in Brysbaert & Stevens [57] for mixed effects models. Cohen's *d* can be interpreted as a standardized mean difference between conditions; according to convention, $d \cong 0.2$ is considered a small effect, $d \cong 0.5$ is considered a medium effect and $d > 0.8$ considered a large effect [58].

Results

Across the three experiments, participants found kTMP stimulation to be tolerable and, indeed, as described below, essentially imperceptible. No adverse events occurred, and no discharges were observed in the EMG after kTMP stimulation.

In each experiment, five TMS probe blocks were sandwiched around active or sham kTMP stimulation (Fig 3). We pooled the data across the two pre-kTMP probe blocks to establish a baseline measure. The post stimulation blocks assessed changes in neural excitability at three time points after kTMP stimulation, operationalized as average percent change post kTMP relative to baseline.

Single Pulse Assay

Non-Modulated kTMP

In Exp 1, we compared three carrier frequencies (2 kHz, 3.5 kHz and 5 kHz) to a sham kTMP condition (0.01 V/m, 3.5 kHz). Exps 2 and 3 included the same non-modulated 3.5 kHz condition (and sham), providing an opportunity for evaluating reproducibility and a reference point for assessing the effect of AM kTMP (see below).

We first tested if the change in corticospinal excitability for the 3.5 kHz condition varied across the three experiments. Using a mixed effect model with fixed factor of Experiment and random effect of Participant we found no difference across the three experiments for the non-modulated 3.5 kHz condition [$\chi^2(2) = 0.41$ $p = 0.813$]. Similarly, we found no difference across experiments for the sham condition [$\chi^2(2) = 2.77$ $p = 0.251$; Fig 4A]. Based on these results, we combined the data across the three experiments for these two conditions in subsequent analyses. Figure 4B displays change in MEP amplitude across the three post kTMP blocks for sham and the 3.5 kHz condition for the three experiments.

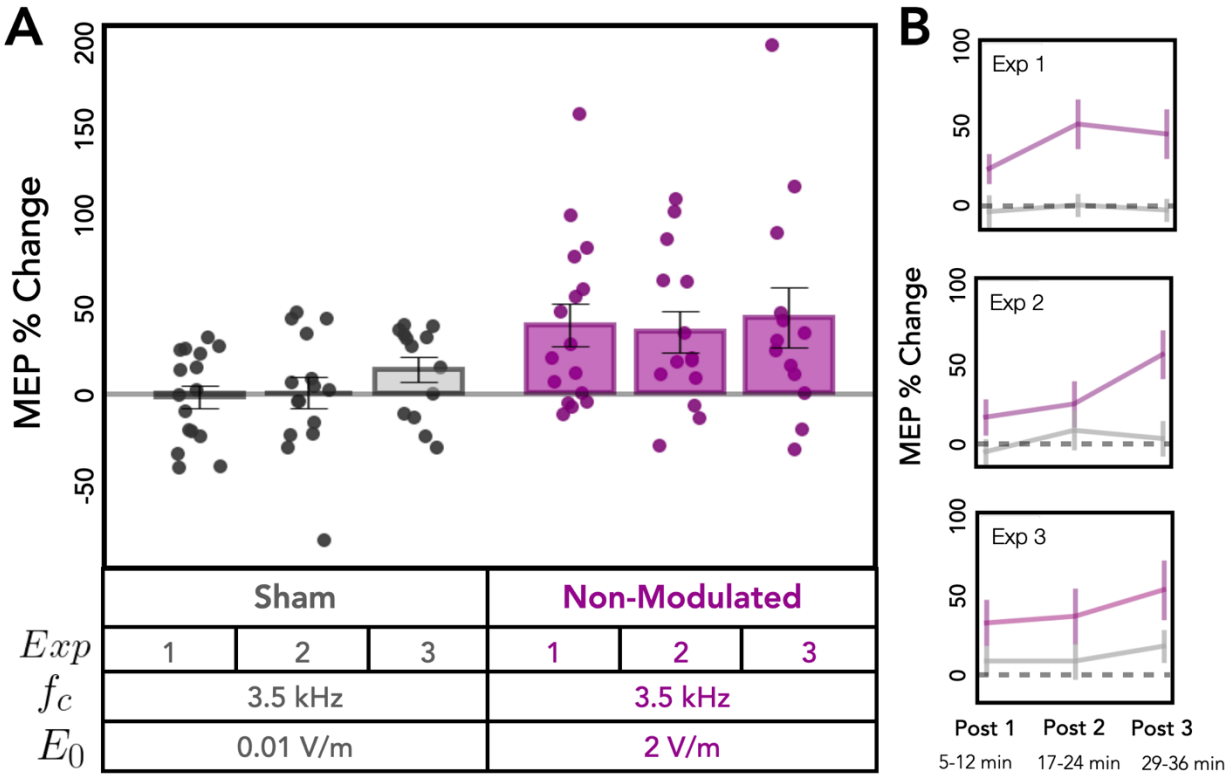

Figure 4. Replication of post-stimulation change in cortical excitability for sham and non-modulated 3.5 kHz kTMP stimulation. A. Change in MEP amplitude measured with single pulse TMS following sham stimulation (left) and kTMP stimulation at 3.5 kHz (right). Dots denote values for individual subjects, bars—mean values, and whiskers—standard error. MEP change post-intervention did not significantly differ across experiments for sham and 3.5 kHz. **B**. Change in MEP amplitude for the three post kTMP blocks for the 3.5 kHz condition (mean ± standard error).

We next compared sham vs. active non-modulated kTMP and found that active kTMP produced a significant increase in corticospinal excitability [$\chi^2(1) = 23.46$ $p < 0.001$; d = 0.50]. Pairwise comparisons of each active condition to sham showed that an increase was observed following both 2 kHz [$\chi^2(1) = 7.02$, $p = 0.008$; $d = 0.43$] and 3.5 kHz kTMP [$\chi^2(1) = 37.75$, $p < 0.001$; $d = 0.69$; Fig 5: Non-Modulated conditions]. The 5 kHz condition failed to reach significance [$\chi^2(1) = 2.52$, $p = 0.113$; $d = 0.25$]. A comparison of the three active conditions showed that the effect on MEP amplitude was influenced by carrier fre-

quency [$\chi^2(1) = 7.31$ $p = 0.026$]. Specifically, the 3.5 kHz condition produced a larger increase in MEP amplitude compared to the 5 kHz condition [$\chi^2(1) = 5.66$ $p = 0.017$; $d = 0.38$]. No difference was observed between the 2 kHz and 3.5 kHz conditions [$\chi^2(1) = 3.02$ $p = 0.082$; $d = 0.25$] or between the 2 kHz and 5 kHz conditions [$\chi^2(1) = 1.36$ $p = 0.244$; $d = 0.21$].

The effect of active non-modulated kTMP stimulation persisted across 36 min of the post-stimulation probe blocks. There was no significant effect of Time (i.e., Post Block) on MEP amplitude [$\chi^2(2) = 5.78$ $p = 0.056$] nor was there a significant interaction between Time and Stimulation Condition [$\chi^2(6) = 9.96$ $p = 0.126$; Fig 6: Non-Modulated conditions].

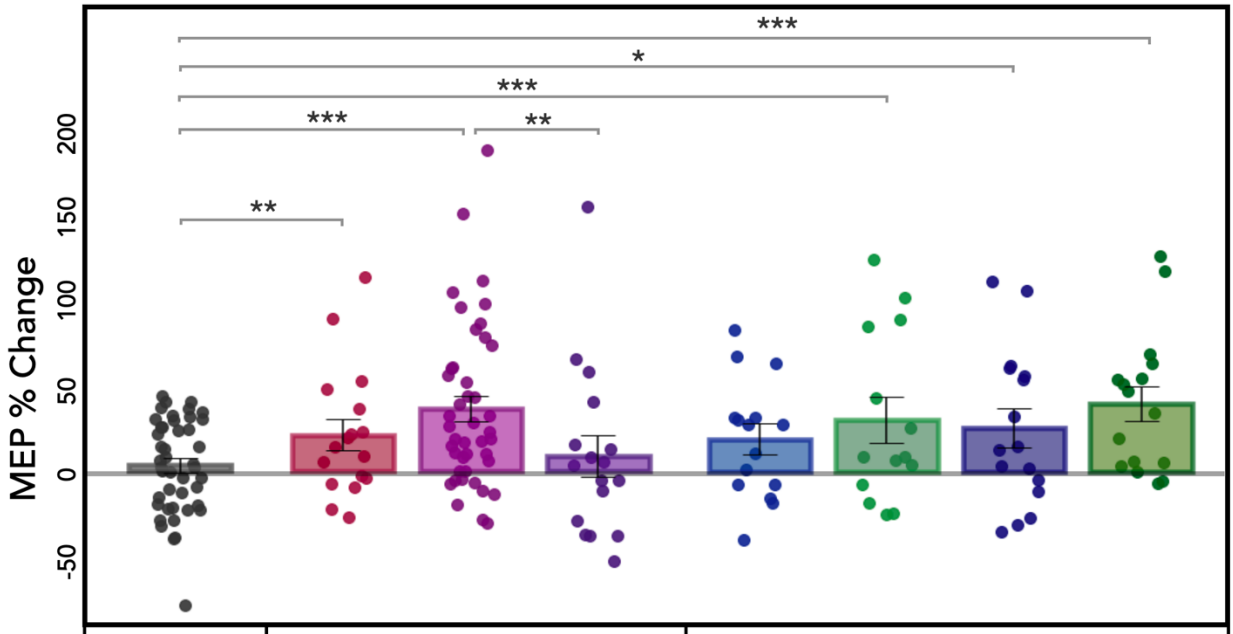

	Sham	Non-Modulated			Amplitude-Modulated			
Exp	1,2,3	1	1,2,3	1	3	2	3	2
f_c	3.5 kHz	2 kHz	3.5 kHz	5 kHz	3.5 kHz			
f_m	0	0	0	0	20	20	140	140
f_b	0	0	0	0	20	40	140	280

Figure 5. Post-stimulation changes in cortical excitability as measured by single-pulse TMS for all conditions. Percent change in MEP amplitude following sham and active kHz stimulation, relative to baseline. Dots denote values for individual subjects, bars—mean values, and whiskers—standard error. Note that the data for the Sham and non-modulated 3.5 kHz conditions are combined across the three experiments. * $p < .05$, ** $p < .01$, *** $p < .001$.

Amplitude-modulated kTMP

We tested the effect of AM kTMP in Exps 2 and 3, with the two experiments using different forms of amplitude modulation (E_{AM1} and E_{AM2}; see Fig 2). For these experiments, we used a carrier frequency of 3.5 kHz given that this condition had produced the largest effect in Exp 1.

Similar to what we observed with non-modulated 3.5 kHz stimulation, AM kTMP resulted in an increase in MEP amplitude compared to sham [$\chi^2(1) = 23.59$ $p < 0.001$; $d = 0.54$; Fig 5, AM conditions]. Pairwise comparisons showed that this effect was observed in three of the four AM conditions: E_{AM1} [$f_m = 20, f_b = 40$; $\chi^2(1) = 17.23$ $p < 0.001$; $d = 0.72$], E_{AM2} [$f_m = 140, f_b = 140$; $\chi^2(1) = 5.30$ $p = 0.021$; $d = 0.39$] and E_{AM1} [$f_m = 140, f_b = 280$; $\chi^2(1) = 28.54$ $p < 0.001$; $d = 0.94$]. The E_{AM2} condition [$f_m = 20, f_b = 20$] showed a numeric increase, but this comparison was not significant [$\chi^2(1) = 2.12$ $p = 0.145$; $d = 0.26$].

Limiting our analysis to the four active AM conditions, we found that MEP amplitude was not dependent on modulating frequency [f_m: $\chi^2(1) = 2.33$ $p = 0.127$] or burst repetition frequency [f_b: $\chi^2(3) = 3.92$ $p = 0.27$]. We found an effect of Time (i.e., Post Block) on MEP amplitude across all conditions [$\chi^2(2) = 6.35$ p = 0.042], but no significant interaction

between Post Block and Stimulation condition [$\chi^2(8) = 5.88$ p = 0.661]. Pairwise comparisons showed that MEP amplitude was greater in Post Block 3 compared to Post Block 1 [$\chi^2(1) = 6.18$ p = 0.013; Fig 6: AM conditions]. No other comparisons were significant [all χ^2's < 2.30, all p's > 0.129].

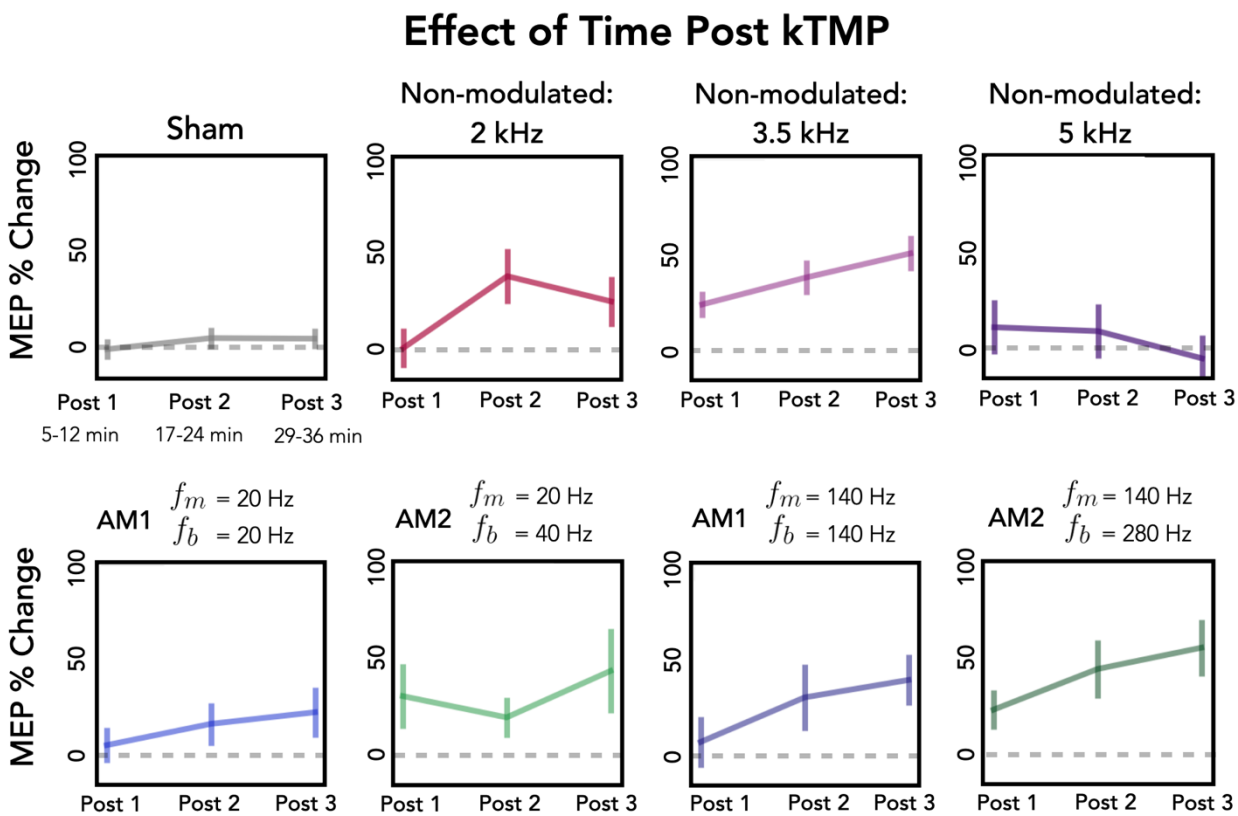

Figure 6. Post-stimulation change in cortical excitability as measured by single-pulse TMS across the three post-kTMP blocks. Percent change in MEP amplitude following sham and active kHz stimulation, relative to baseline for the three post blocks (error bars represent standard error). The data for the Sham and non-modulated 3.5 kHz conditions are combined across the three experiments.

Our main interest in the AM conditions is to determine if amplitude modulation at physiologically relevant frequencies produces a change on cortical excitability beyond that produced by the kHz carrier frequency. To this end, we compared the effect of AM kTMP to non-modulated kTMP, with the latter limited to the 3.5 kHz condition (pooled data). Using a mixed effect model, this contrast was not significant [$\chi^2(1) = 1.57$ $p = 0.210$; $d = 0.14$].

Thus, the AM conditions provide another demonstration that kHz stimulation can increase cortical excitability; however, at least with a 2 V/m E-field, we did not observe an effect from the AM component that was above and beyond non-modulated kTMP.

Paired-Pulse Assays

We included two paired-pulse assays that provide probes of intracortical inhibition or facilitation. To confirm that we observed SICI, we focused on the pre-kTMP data, thus avoiding any influence from kTMP stimulation. We pooled the data across the two pre-kTMP blocks for each individual and performed an analysis on the data from the participants from Exps 1 and 2. This analysis showed a strong SICI effect, with a mean decrease of 36% on the paired-pulse trials relative to the single pulse trials [$t(125) = -24.47$, $p < .001$; Fig 7]. A similar level of attenuation was observed in the post-kTMP blocks following sham stimulation.

We then asked if the magnitude of SICI effect was modulated by kTMP. Compared to sham, we observed no effect of active non-modulated kTMP [$\chi^2(1) = 1.12$, $p = 0.289$], no effect of post-stimulation block [$\chi^2(2) = 0.51$, $p = 0.773$] and no interaction between these two factors [$\chi^2(6) = 5.46$, $p = 0.486$]. Similarly, there was no effect of active AM kTMP on SICI (relative to sham) [$\chi^2(1) = 0.81$, $p = 0.369$], no effect of post-stimulation block [$\chi^2(2) = 0.39$, $p = 0.823$] and no interaction between the two factors [$\chi^2(4) = 4.17$, $p = 0.383$]. In sum, kTMP does not appear to influence the magnitude of intracortical inhibition measured by the paired-pulse test.

The second paired-pulse assay was designed to examine intracortical facilitation (ICF). In the baseline, pre-kTMP blocks, the MEP amplitude was greater in this paired-pulse condition compared to the single pulse protocol, with a mean facilitation effect of 22% [$t(125) = 6.86$, $p < .001$; Fig 6].

As with SICI, there was no evidence that kTMP influenced ICF: We found no effect of active non-modulated kTMP compared to sham [$\chi^2(1) = 1.15$, $p = 0.283$], no effect of post-stimulation block [$\chi^2(2) = 1.46$, $p = 0.482$], and no interaction between the two factors [$\chi^2(6) = 5.04$, $p = 0.539$]. Similarly, we found no effect of active AM kTMP compared to sham [$\chi^2(1) = 0.73$, $p = 0.391$], no effect of post-stimulation block [$\chi^2(2) = 0.72$, $p = 0.699$] and no interaction between the two factors [$\chi^2(4) = 2.45$, $p = 0.655$].

In summary, kTMP, either non-modulated or amplitude modulated at 2 V/m, did not produce any measurable effect on the paired-pulse assays of intracortical inhibition or facilitation, SICI and ICF.

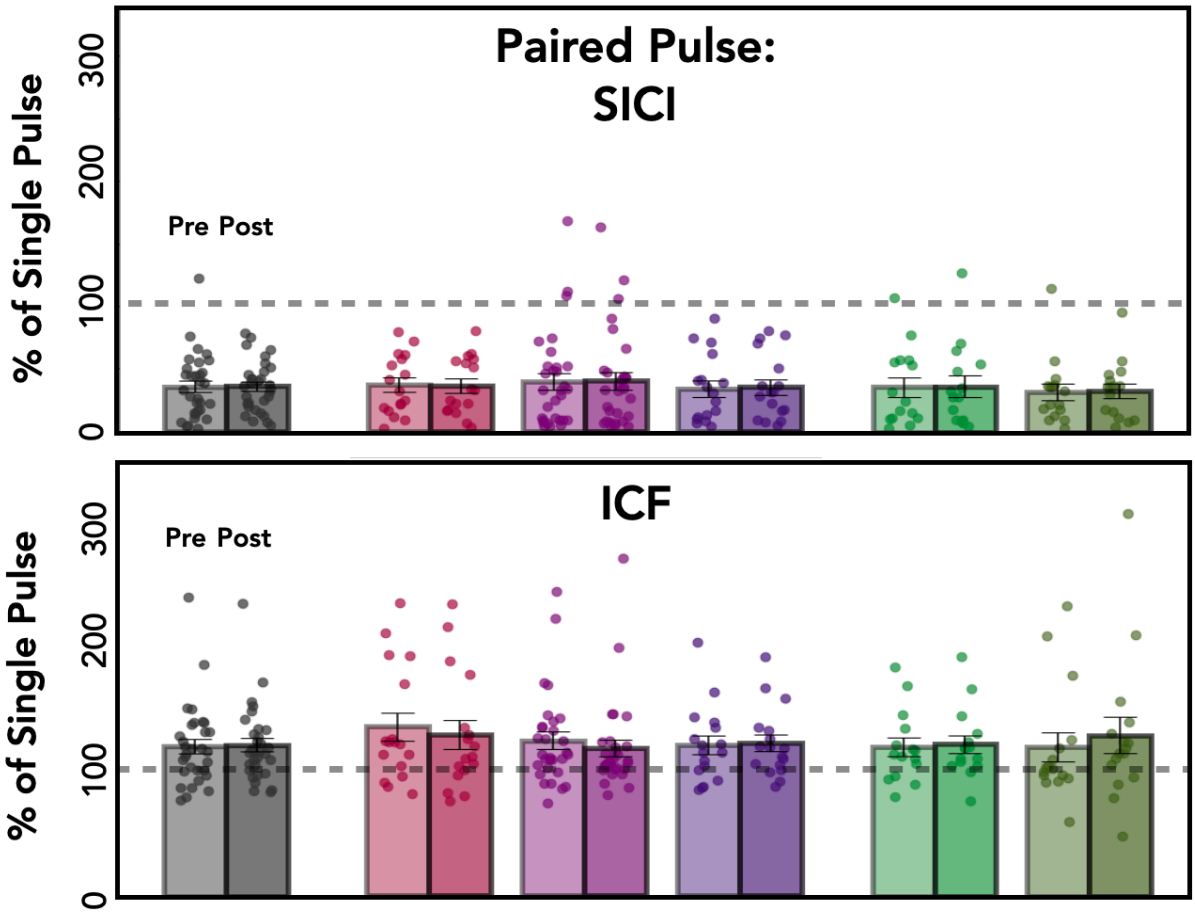

	Sham	Non-Modulated			Amplitude-Modulated	
Exp	1	1	1,2	1	2	2
f_c	3.5 kHz	2 kHz	3.5 kHz	5 kHz	3.5 kHz	
f_m	0	0	0	0	20	140
f_b	0	0	0	0	40	280

Figure 7. kTMP did not produce any change in measures of short intracortical inhibition or intracortical facilitation. Data are plotted as the ratio of the paired-pulse MEP amplitude over the single pulse MEP amplitude, with an inter-pulse interval of 3 ms for SICI and 10 ms for ICF. Each pair of bars shows this ratio for pre-kTMP (averaged over two probe blocks) and post-kTMP (averaged over three probe blocks).

Subjective experience during kTMP stimulation

Informal observations from the participants in Exp 1 indicated that the coil did not produce any detectable tactile sensation. The amplifier produces a sound, but one that was effectively masked by playing a louder, pre-recorded sound (3.5 kHz tone) in all conditions.

Participants provided three ratings using an 11-point scale (0 = not at all; 10 = extremely) in response to questions on annoyance, pain, and subjective experience of muscle activation/movement. Figure 8 presents the data for each measure following TMS, active kTMP, and sham kTMP. In line with expectations for TMS [48], the participants were aware of muscle twitches, but the stimulation was well-tolerated in terms of annoyance and pain given that the coil was positioned over primary motor cortex.

Of primary interest for the present report, the modal rating was 0 for all three ratings following active kTMP. Using a mixed effects model, with a fixed factor of Stimulation type (i.e., active vs. sham) and Participant as a random effect, we found no difference between active and sham kTMP for Annoyance [$\chi^2(1) = 0.17$, $p = 0.675$], Pain [$\chi^2(1) = 0.32$, $p = 0.573$] and the subjective experience of Muscle Twitches [$\chi^2(1) = 0.01$, $p = 0.972$]. Some participants rated active and sham kTMP high in terms of annoyance. Based on open ended survey responses these scores appear to be related to general features of the experiment such as tension from the neuronavigation headband and the requirement to maintain a sitting posture for an extended period. In summary, the survey data and subjective reports suggest that kTMP is well suited for double-blind experimentation.

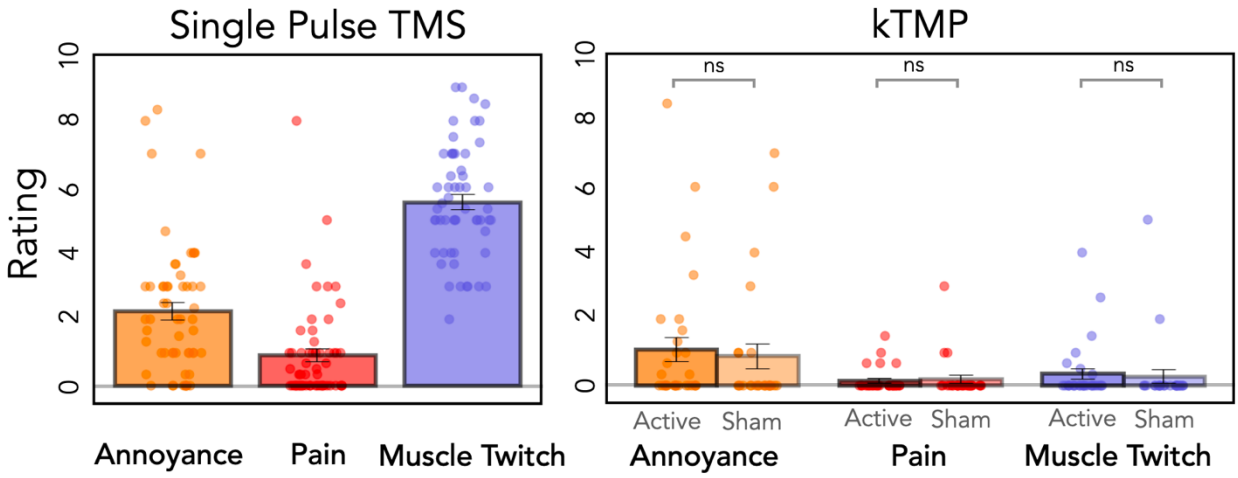

Figure 8. kTMP stimulation is not associated with any subjective experience. Mean ratings (SE in parenthesis) combined across Exp 2 and Exp 3 on a 0-to-10 scale in response to questions assessing annoyance, pain, and awareness of finger movement. For TMS, the survey was administered after the second baseline probe block; for kTMP, the survey was administered after kTMP stimulation.

Discussion

In this paper, we present a new method, kTMP, for exploring the subthreshold NIBS experimental space. The kTMP E-field has the waveform flexibility of kilohertz tES along with the potential amplitude range and focality of TMS. Moreover, amplitude modulation of the kTMP E-field yields a waveform which could potentially introduce stimulation dynamics at frequencies matching endogenous neural rhythms (e.g., alpha, beta).

Summary of experimental findings and limitations

Across three experiments, we assessed the ability of non-modulated and amplitude-modulated kTMP to alter cortical excitability, using suprathreshold TMS over motor cortex to elicit MEPs in a finger muscle. In Experiment 1, non-modulated kTMP with a targeted cortical E-field of 2 V/m, produced an increase in corticospinal excitability at 2 and 3.5 kHz. The latter condition also resulted in a larger increase in MEP amplitude compared to stimulation at 5 kHz, suggesting a possible effect of carrier frequency. Experiments 2

and 3 provided replications of the efficacy of non-modulated kTMP at 3.5 kHz to increase corticospinal excitability. Importantly, participants experienced no tactile sensation or discomfort from the procedure. Indeed, the only percept of kTMP at 2.0 V/m is a tone at the carrier frequency emanating from the amplifier. This sound was masked in our experiments by a background tone played during active and sham kTMP stimulation.

Due to pandemic related university regulations, we were limited to a two-hour experimental session. As such, we were only able to assess the impact of kTMP on neural excitability in three probe blocks, spanning a 36 min post-stimulation epoch. We did not observe a reduction of the kTMP effect across this window. Future testing with extended post-stimulation assays will be required to establish the duration of the effect of kTMP on cortical excitability.

We also tested two forms of AM, using modulation frequencies of 20 Hz and 140 Hz. An increase in corticospinal excitability was observed in three of the four conditions, associated with high burst repetition frequencies. Critically, none of the AM kTMP conditions produced an increase above that observed with non-modulated 3.5 kHz kTMP, suggesting that at least for an E-field amplitude of 2 V/m, amplitude modulation at physiologically-relevant frequencies does not induce an additional lasting change in corticospinal excitability over that arising from the kHz carrier frequency alone.

Despite the absence of an effect from amplitude modulation, the present results are encouraging in that, across a range of conditions, we consistently observed an increase in

cortical excitability in response to single-pulse TMS following the application of a 2 V/m E-field for 10 min. On average the increase in MEP amplitude following 3.5 kHz non-modulated kTMP with a cortical E-field of 2 V/m, the condition in which we have the largest sample size, was 37%. This value is in the range observed in studies using a variety of NIBS methods and protocols [20,59,60].

Potential mechanisms of kTMP

At present, we can only tentatively speculate about how kTMP modulates cortical excitability. As with other NIBS modalities, a mechanistic understanding would address (1) what cellular element is directly perturbed, (2) which cortical neurons are modulated, and (3) how modulation confers lasting cortical excitability. We discuss these questions below.

Regarding acute effects, suprathreshold TMS activates neurons by inducing a brief E-field pulse with dominant frequency component in the kilohertz range (2–6 kHz) [61], demonstrating that such frequencies can acutely affect neuronal polarization. While the slower time constants of the soma and dendrite membranes mostly filter out kilohertz frequencies, the faster time constants of the axonal membrane allow kilohertz waveforms to produce transient polarization in the axons, especially axonal (presynaptic) terminals [62–66]. Whereas suprathreshold TMS pulses induce action potentials in the axons, kTMP would only produce subthreshold perturbation of the axonal membrane potential. Thus, the effects of kTMP may be mediated by acute subthreshold polarization perturbation of presynaptic terminals.

Regarding the modulation of specific cortical circuits, the single-pulse and paired-pulse TMS measurements can provide some insights; it has to be recognized, however, that these results depend on both the intervention (kTMP) as well as the TMS probe characteristics. The shape of the TMS pulse and coil orientation impact how a suprathreshold TMS pulse elicits an MEP: The MEP can come about via direct excitation of the axons of the corticospinal neurons (D-wave), via indirect effects on neurons that provide synaptic input to corticospinal neurons (I-waves) or a combination of both. We applied the TMS probes using suprathreshold biphasic TMS pulses with a posterior–anterior dominant induced current. At the probing stimulation level (120% rMT), this configuration has been shown to preferentially recruit I-waves [67]. Moreover, since kTMP used the same coil configuration, it can be inferred that the kTMP E-field coupled most strongly to the same neural elements as the TMS probing pulses. Assuming that we are unable to probe the impact of kTMP on D-waves, we can speculate that the plasticity induced by kTMP predominantly affects excitatory synaptic inputs to pyramidal tract neurons. This mechanistic hypothesis is similar to that proposed for intermittent theta burst stimulation (iTBS), another sub-threshold magnetic induction protocol that produces a temporally extended increase in single-pulse MEPs [68]. However, it will be important to employ alternative coil configurations in future research to assess if kTMP can modulate the excitability of D-waves, representing direct activation of the axons of pyramidal tract neurons.

We did not observe any effect of kTMP on the two paired-pulse protocols, SICI and ICF. They appear to probe, respectively, GABA-mediated inhibitory and glutamate-mediated excitatory cortical circuits [44]. Although we observed the classic signatures of SICI and

ICF, kTMP did not modulate either of these measures of local intracortical neural dynamics. This pattern matches that observed with iTBS: A meta-analysis of iTBS studies failed to find consistent changes in SICI or ICF despite a consistent increase in single-pulse MEPs [46]. In contrast, a meta-analysis of anodal tDCS revealed an increase in single-pulse MEP amplitude, a decrease in SICI, and an increase in ICF [69]. Interestingly, tACS at 20 Hz also produced a similar pattern on all three measures in a phase-dependent manner during stimulation [70]. It is notable that kTMP and iTBS share the same spatial distribution of the E-field (determined by the TMS coil configuration), which is very different from that of the electrical stimulation with tDCS and tACS. Moreover, both TMS and kTMP involve stimuli in the kHz spectrum whereas tDCS and 20 Hz tACS use E-fields that vary on slower time scales. This variation can result in a different pattern of polarization across neural elements. The overlapping characteristics shared by kTMP and iTBS may account for the similarity in coupling to specific cortical circuits which differ from those affected by tDCS and low frequency tACS.

Finally, we can consider different hypotheses concerning how kHz stimulation produces changes in neuronal activity lasting beyond the stimulus train. One possibility is that the continuous acute perturbation of the presynaptic terminals interacts with the endogenous axonal signaling, for example via stochastic resonance, ultimately causing synaptic potentiation [71]. Another option is that the nonlinear properties of the neuronal membrane lead to temporal summation of successive kilohertz subthreshold cycles and, consequently, a facilitation of synaptic transmission [16]. The repeated perturbation of the neuronal membrane could also result in accumulation of calcium in presynaptic terminals, yielding synaptic plasticity effects [20]. Presently, these possibilities are speculative and

need to be assessed by further research into the cellular mechanisms of subthreshold kilohertz neuromodulation.

Methodological advantages of kTMP

A limiting factor for tES studies is that these methods are restricted to the very low end of subthreshold space in terms of E-field amplitude. Thus, there is a limited range over which one could obtain dose-dependent effects; indeed, efforts to establish dose-dependent response functions with NIBS protocols have provided mixed results [41,42]. In contrast, kTMP has the potential to open a large subthreshold experimental space, one that has considerable range in terms of E-field amplitude, carrier frequency, AM waveform, and stimulation duration. We should be able to achieve at least a 4-fold increase in the kTMP cortical E-field amplitude (e.g., up to 8 V/m in the kHz range) [10,17] without uncomfortable scalp stimulation. This expanded parameter space, especially in terms of E-field amplitude should prove beneficial in deriving dose-dependent response functions. Theoretically, kTMP could reach suprathreshold E-field amplitudes although moving into that space will require careful assessment of issues related to power requirements, coil heating, acoustic noise, and participant safety.

In addition to offering a large subthreshold experimental space, there are other noteworthy features of kTMP. First, kTMP is ideally suited for double-blind experimentation. As verified in the subjective reports of our participants, the only percept associated with 2.0 V/m kTMP is a tone at the carrier frequency emanating from the amplifier, one that can be masked. Informally, we have placed the coil at different locations on the scalp and

found that, even when positioned over inferior prefrontal or occipital cortex, there is no scalp stimulation or tactile percept from kTMP stimulation, issues that can impact TMS and tES protocols [48,72].

Second, for studies using TMS as a probe of NIBS efficacy, the E-fields of the perturbation (e.g., kTMP) and probe (e.g., suprathreshold single-pulse TMS) have matched spatial distribution and only differ in terms of their waveforms and strengths. In contrast, the E-fields of tES and TMS cannot be matched [10] and, as such, likely impact different neural populations even when the targeted region is ostensibly the same. Beyond the experimental convenience of using the same TMS coil for both perturbation and probe as in our prototype, the E-field alignment may increase experimental robustness.

Third, the experimenter can create a kTMP waveform of unlimited flexibility. For example, using AM kTMP to introduce perturbations at physiologically relevant frequencies could provide a method to enhance plasticity or even induce neural entrainment. Although we failed to observe an additional effect of AM kTMP, research using non-human models suggests that entrainment effects from NIBS requires strong E-fields since the exogenous stimulation pattern must compete with endogenous brain rhythms [9,17,73]. As such, kTMP offers an approach that combines an expanded range of subthreshold E-field amplitudes with waveform flexibility in the kHz range.

Fourth, E-fields produced through magnetic induction, unlike tES E-fields, depend weakly upon the distribution of tissue conductivity - estimates of which vary widely in the literature

[74]. Indeed, for spherical shell head models the E-field produced through magnetic induction is independent of conductivity—something that does not hold for tES E-fields. This should reduce variability when modeling the E-field based on individualized head geometry.

Fifth, as with other NIBS methods [75–78] we anticipate that simultaneous EEG and kTMP will enable the investigation of the evolution of neural effects in real-time. For example, with amplitude modulated kTMP the artifact from the kHz carrier frequency can be removed, albeit with possible technical hurdles connected to nonlinearities associated with presently available recording and stimulation hardware [79]. This approach could be used to tailor the stimulation waveform on an individual basis or for closed-loop control, promising avenues for translational applications of NIBS.

Conclusion

In conclusion kTMP offers an opportunity to explore a new experimental space, one with a relatively large range of subthreshold E-field induction, the focality of TMS, and the potential to impose E-fields at physiological relevant frequencies, with significantly less tolerability issues than tES or suprathreshold TMS.

Acknowledgements

We are grateful to our team of research assistants, Tatianna Howard, Alice Wang, Serena Chi, Caroline Cao, Lauren Anne Schuck, Emily Schultz, Carolyn Irving, Lizzy Trinh, Kevin Peter, Owen Doyle and Connor Brown. Assaf Breska provided advice on the statistical analyses. This work was supported by grants from the NIH (R21 EB028075; R35 NS116883; 1R44 NS127667) and NSF (EAGER 1946316) and intramural funding from the Henry H. Wheeler, Jr. Brain Imaging Center. We thank MagVenture for providing the TMS stimulator and coil used in this study.

Author contributions

D.S., L.L., R.B.I. and B.I. conceived the project. D.S. designed and developed kTMP. L.L. and R.B.I designed the TMS experiments. L.L. and C.M. coordinated the data collection and C.M. performed the data and statistical analyses. A.V.P. contributed to the experiment design and data analysis and interpretation. L.L., D.S., and C.M. drafted the paper, and all authors participated in the editing process. All authors approve the final version of the manuscript and are accountable for all aspects of the work. All persons designated as authors qualify for authorship, and all those who qualify for authorship are listed.

Conflict of Interest

The authors declare the following competing interests: LL, CM, BI, RBI and DS have stock ownership and AVP is a paid consultant of Magnetic Tides, a non-publicly traded company created to develop new methods of non-invasive brain stimulation. UC Berkley holds

the patent rights related to the kTMP technology and has provided Magnetic Tides with an exclusive licensing agreement.

Data availability

The data used to support the results are available upon request from the corresponding author.

References

[1] Polanía R, Nitsche MA, Ruff CC. Studying and modifying brain function with non-invasive brain stimulation. Nat Neurosci 2018;21:174–87. https://doi.org/10.1038/s41593-017-0054-4.

[2] Di Lazzaro V, Bella R, Benussi A, Bologna M, Borroni B, Capone F, et al. Diagnostic contribution and therapeutic perspectives of transcranial magnetic stimulation in dementia. Clin Neurophysiol 2021;132:2568–607. https://doi.org/10.1016/j.clinph.2021.05.035.

[3] Fitzgerald PB. An update on the clinical use of repetitive transcranial magnetic stimulation in the treatment of depression. J Affect Disord 2020;276:90–103. https://doi.org/10.1016/j.jad.2020.06.067.

[4] Grigoras I-F, Stagg CJ. Recent advances in the role of excitation-inhibition balance in motor recovery post-stroke. Fac Rev 2021;10:58. https://doi.org/10.12703/r/10-58.

[5] Iglesias AH. Transcranial Magnetic Stimulation as Treatment in Multiple Neurologic Conditions. Curr Neurol Neurosci Rep 2020;20:1. https://doi.org/10.1007/s11910-020-1021-0.

[6] Lefaucheur J-P, Aleman A, Baeken C, Benninger DH, Brunelin J, Di Lazzaro V, et al. Evidence-based guidelines on the therapeutic use of repetitive transcranial magnetic stimulation (rTMS): An update (2014-2018). Clin Neurophysiol 2020;131:474–528. https://doi.org/10.1016/j.clinph.2019.11.002.

[7] Maatoug R, Bihan K, Duriez P, Podevin P, Silveira-Reis-Brito L, Benyamina A, et al. Non-invasive and invasive brain stimulation in alcohol use disorders: A critical review of selected human evidence and methodological considerations to guide future research. Compr Psychiatry 2021;109:152257. https://doi.org/10.1016/j.comppsych.2021.152257.

[8] Huang Y-Z, Lu M-K, Antal A, Classen J, Nitsche M, Ziemann U, et al. Plasticity induced by non-invasive transcranial brain stimulation: A position paper. Clin Neurophysiol 2017;128:2318–29. https://doi.org/10.1016/j.clinph.2017.09.007.

[9] Liu A, Vöröslakos M, Kronberg G, Henin S, Krause MR, Huang Y, et al. Immediate neurophysiological effects of transcranial electrical stimulation. Nature Communications 2018;9:5092. https://doi.org/10.1038/s41467-018-07233-7.

[10] Sheltraw D, Inglis B, Labruna L, Ivry R. Comparing the electric fields of Transcranial electric and magnetic perturbation. J Neural Eng 2021. https://doi.org/10.1088/1741-2552/abebee.

[11] Alekseichuk I, Mantell K, Shirinpour S, Opitz A. Comparative modeling of transcranial magnetic and electric stimulation in mouse, monkey, and human. Neuroimage 2019;194:136–48. https://doi.org/10.1016/j.neuroimage.2019.03.044.

[12] Huang Y, Liu AA, Lafon B, Friedman D, Dayan M, Wang X, et al. Correction: Measurements and models of electric fields in thein vivohuman brain during transcranial electric stimulation. Elife 2018;7. https://doi.org/10.7554/eLife.35178.

[13] Vöröslakos M, Takeuchi Y, Brinyiczki K, Zombori T, Oliva A, Fernández-Ruiz A, et al. Direct effects of transcranial electric stimulation on brain circuits in rats and humans. Nat Commun 2018;9:483. https://doi.org/10.1038/s41467-018-02928-3.

[14] Hsu G, Farahani F, Parra LC. Cutaneous Sensation of Electrical Stimulation Waveforms. Brain Stimul 2021;14:693–702. https://doi.org/10.1016/j.brs.2021.04.008.

[15] Esmaeilpour Z, Kronberg G, Reato D, Parra LC, Bikson M. Temporal interference stimulation targets deep brain regions by modulating neural oscillations. Brain Stimul 2021;14:55–65. https://doi.org/10.1016/j.brs.2020.11.007.

[16] Neudorfer C, Chow C, Boutet A, Loh A, Germann J, Elias GJ, et al. Kilohertz-frequency stimulation of the nervous system: a review of underlying mechanisms. Brain Stimulation: Basic, Translational, and Clinical Research in Neuromodulation 2021;0. https://doi.org/10.1016/j.brs.2021.03.008.

[17] Wang B, Aberra AS, Grill WM, Peterchev AV. Responses of model cortical neurons to temporal interference stimulation and related transcranial alternating current stimulation modalities. J Neural Eng 2023;19. https://doi.org/10.1088/1741-2552/acab30.
[18] Bhadra N, Foldes E, Vrabec T, Kilgore K, Bhadra N. Temporary persistence of conduction block after prolonged kilohertz frequency alternating current on rat sciatic nerve. J Neural Eng 2018;15:016012. https://doi.org/10.1088/1741-2552/aa89a4.
[19] Grossman N, Bono D, Dedic N, Kodandaramaiah SB, Rudenko A, Suk H-J, et al. Noninvasive Deep Brain Stimulation via Temporally Interfering Electric Fields. Cell 2017;169:1029-1041.e16. https://doi.org/10.1016/j.cell.2017.05.024.
[20] Chaieb L, Antal A, Paulus W. Transcranial alternating current stimulation in the low kHz range increases motor cortex excitability. Restor Neurol Neurosci 2011;29:167–75. https://doi.org/10.3233/RNN-2011-0589.
[21] Chaieb L, Antal A, Pisoni A, Saiote C, Opitz A, Ambrus GG, et al. Safety of 5 kHz tACS. Brain Stimul 2014;7:92–6. https://doi.org/10.1016/j.brs.2013.08.004.
[22] Wang B, Shen MR, Deng Z-D, Smith JE, Tharayil JJ, Gurrey CJ, et al. Redesigning existing transcranial magnetic stimulation coils to reduce energy: application to low field magnetic stimulation. J Neural Eng 2018. https://doi.org/10.1088/1741-2552/aaa505.
[23] Rohan ML, Yamamoto RT, Ravichandran CT, Cayetano KR, Morales OG, Olson DP, et al. Rapid mood-elevating effects of low field magnetic stimulation in depression. Biol Psychiatry 2014;76:186–93. https://doi.org/10.1016/j.biopsych.2013.10.024.
[24] Carlezon WA, Rohan ML, Mague SD, Meloni EG, Parsegian A, Cayetano K, et al. Antidepressant-like effects of cranial stimulation within a low-energy magnetic field in rats. Biol Psychiatry 2005;57:571–6. https://doi.org/10.1016/j.biopsych.2004.12.011.
[25] Rohan M, Parow A, Stoll AL, Demopulos C, Friedman S, Dager S, et al. Low-field magnetic stimulation in bipolar depression using an MRI-based stimulator. Am J Psychiatry 2004;161:93–8. https://doi.org/10.1176/appi.ajp.161.1.93.
[26] Dubin MJ, Ilieva IP, Deng Z-D, Thomas J, Cochran A, Kravets K, et al. A double-blind pilot dosing study of low field magnetic stimulation (LFMS) for treatment-resistant depression (TRD). J Affect Disord 2019;249:286–93. https://doi.org/10.1016/j.jad.2019.02.039.
[27] Volkow ND, Tomasi D, Wang G-J, Fowler JS, Telang F, Wang R, et al. Effects of low-field magnetic stimulation on brain glucose metabolism. Neuroimage 2010;51:623–8. https://doi.org/10.1016/j.neuroimage.2010.02.015.
[28] Huang Y-Z, Edwards MJ, Rounis E, Bhatia KP, Rothwell JC. Theta burst stimulation of the human motor cortex. Neuron 2005;45:201–6. https://doi.org/10.1016/j.neuron.2004.12.033.
[29] Nitsche MA, Seeber A, Frommann K, Klein CC, Rochford C, Nitsche MS, et al. Modulating parameters of excitability during and after transcranial direct current stimulation of the human motor cortex. J Physiol (Lond) 2005;568:291–303. https://doi.org/10.1113/jphysiol.2005.092429.
[30] Nitsche MA, Paulus W. Sustained excitability elevations induced by transcranial DC motor cortex stimulation in humans. Neurology 2001;57:1899–901. https://doi.org/10.1212/WNL.57.10.1899.
[31] Nitsche MA, Paulus W. Excitability changes induced in the human motor cortex by weak transcranial direct current stimulation. J Physiol (Lond) 2000;527 Pt 3:633–9.
[32] Lu H, Lam LCW, Ning Y. Scalp-to-cortex distance of left primary motor cortex and its computational head model: Implications for personalized neuromodulation. CNS Neurosci Ther 2019;25:1270–6. https://doi.org/10.1111/cns.13204.
[33] Nieminen JO, Koponen LM, Ilmoniemi RJ. Experimental Characterization of the Electric Field Distribution Induced by TMS Devices. Brain Stimul 2015;8:582–9. https://doi.org/10.1016/j.brs.2015.01.004.

[34] Feurra M, Pasqualetti P, Bianco G, Santarnecchi E, Rossi A, Rossi S. State-Dependent Effects of Transcranial Oscillatory Currents on the Motor System: What You Think Matters. J Neurosci 2013;33:17483–9. https://doi.org/10.1523/JNEUROSCI.1414-13.2013.
[35] Feurra M, Bianco G, Santarnecchi E, Del Testa M, Rossi A, Rossi S. Frequency-dependent tuning of the human motor system induced by transcranial oscillatory potentials. J Neurosci 2011;31:12165–70. https://doi.org/10.1523/JNEUROSCI.0978-11.2011.
[36] Heise K-F, Kortzorg N, Saturnino GB, Fujiyama H, Cuypers K, Thielscher A, et al. Evaluation of a Modified High-Definition Electrode Montage for Transcranial Alternating Current Stimulation (tACS) of Pre-Central Areas. Brain Stimul 2016;9:700–4. https://doi.org/10.1016/j.brs.2016.04.009.
[37] Dissanayaka T, Zoghi M, Farrell M, Egan GF, Jaberzadeh S. Does transcranial electrical stimulation enhance corticospinal excitability of the motor cortex in healthy individuals? A systematic review and meta-analysis. Eur J Neurosci 2017;46:1968–90. https://doi.org/10.1111/ejn.13640.
[38] Inukai Y, Saito K, Sasaki R, Tsuiki S, Miyaguchi S, Kojima S, et al. Comparison of Three Non-Invasive Transcranial Electrical Stimulation Methods for Increasing Cortical Excitability. Front Hum Neurosci 2016;10:668. https://doi.org/10.3389/fnhum.2016.00668.
[39] Moliadze V, Antal A, Paulus W. Boosting brain excitability by transcranial high frequency stimulation in the ripple range. J Physiol 2010;588:4891–904. https://doi.org/10.1113/jphysiol.2010.196998.
[40] Carroll TJ, Riek S, Carson RG. Reliability of the input-output properties of the cortico-spinal pathway obtained from transcranial magnetic and electrical stimulation. J Neurosci Methods 2001;112:193–202.
[41] Kamen G. Reliability of motor-evoked potentials during resting and active contraction conditions. Med Sci Sports Exerc 2004;36:1574–9.
[42] Malcolm MP, Triggs WJ, Light KE, Shechtman O, Khandekar G, Gonzalez Rothi LJ. Reliability of motor cortex transcranial magnetic stimulation in four muscle representations. Clin Neurophysiol 2006;117:1037–46. https://doi.org/10.1016/j.clinph.2006.02.005.
[43] Rossini PM, Burke D, Chen R, Cohen LG, Daskalakis Z, Di Iorio R, et al. Non-invasive electrical and magnetic stimulation of the brain, spinal cord, roots and peripheral nerves: Basic principles and procedures for routine clinical and research application. An updated report from an I.F.C.N. Committee. Clin Neurophysiol 2015;126:1071–107. https://doi.org/10.1016/j.clinph.2015.02.001.
[44] Cash RFH, Ziemann U. Paired-pulse interactions. In: Wassermann EM, Peterchev AV, Ziemann U, Lisanby SH, Siebner HR, Walsh V, editors. The Oxford Handbook of Transcranial Stimulation, Oxford University Press; n.d., p. 0. https://doi.org/10.1093/oxfordhb/9780198832256.013.13.
[45] Horvath JC, Forte JD, Carter O. Evidence that transcranial direct current stimulation (tDCS) generates little-to-no reliable neurophysiologic effect beyond MEP amplitude modulation in healthy human subjects: A systematic review. Neuropsychologia 2015;66:213–36. https://doi.org/10.1016/j.neuropsychologia.2014.11.021.
[46] Chung SW, Hill AT, Rogasch NC, Hoy KE, Fitzgerald PB. Use of theta-burst stimulation in changing excitability of motor cortex: A systematic review and meta-analysis. Neurosci Biobehav Rev 2016;63:43–64. https://doi.org/10.1016/j.neubiorev.2016.01.008.
[47] Biabani M, Aminitehrani M, Zoghi M, Farrell M, Egan G, Jaberzadeh S. The effects of transcranial direct current stimulation on short-interval intracortical inhibition and intracortical facilitation: a systematic review and meta-analysis. Reviews in the Neurosciences 2018;29:99–114. https://doi.org/10.1515/revneuro-2017-0023.
[48] Meteyard L, Holmes NP. TMS SMART - Scalp mapping of annoyance ratings and twitches caused by Transcranial Magnetic Stimulation. J Neurosci Methods 2018;299:34–44. https://doi.org/10.1016/j.jneumeth.2018.02.008.

[49] Goldsworthy MR, Hordacre B, Ridding MC. Minimum number of trials required for within- and between-session reliability of TMS measures of corticospinal excitability. Neuroscience 2016;320:205–9. https://doi.org/10.1016/j.neuroscience.2016.02.012.
[50] Cavaleri R, Schabrun SM, Chipchase LS. The number of stimuli required to reliably assess corticomotor excitability and primary motor cortical representations using transcranial magnetic stimulation (TMS): a systematic review and meta-analysis. Syst Rev 2017;6:48. https://doi.org/10.1186/s13643-017-0440-8.
[51] Biabani M, Farrell M, Zoghi M, Egan G, Jaberzadeh S. The minimal number of TMS trials required for the reliable assessment of corticospinal excitability, short interval intracortical inhibition, and intracortical facilitation. Neuroscience Letters 2018;674:94–100. https://doi.org/10.1016/j.neulet.2018.03.026.
[52] Peterchev AV, Goetz SM, Westin GG, Luber B, Lisanby SH. Pulse width dependence of motor threshold and input-output curve characterized with controllable pulse parameter transcranial magnetic stimulation. Clin Neurophysiol 2013;124:1364–72. https://doi.org/10.1016/j.clinph.2013.01.011.
[53] Nielsen JF. Improvement of amplitude variability of motor evoked potentials in multiple sclerosis patients and in healthy subjects. Electroencephalogr Clin Neurophysiol 1996;101:404–11.
[54] Nielsen JF. Logarithmic distribution of amplitudes of compound muscle action potentials evoked by transcranial magnetic stimulation. J Clin Neurophysiol 1996;13:423–34. https://doi.org/10.1097/00004691-199609000-00005.
[55] Goetz SM, Luber B, Lisanby SH, Peterchev AV. A novel model incorporating two variability sources for describing motor evoked potentials. Brain Stimul 2014;7:541–52. https://doi.org/10.1016/j.brs.2014.03.002.
[56] Bates D, Mächler M, Bolker B, Walker S. Fitting Linear Mixed-Effects Models Using lme4. Journal of Statistical Software 2015;67:1–48. https://doi.org/10.18637/jss.v067.i01.
[57] Brysbaert M, Stevens M. Power Analysis and Effect Size in Mixed Effects Models: A Tutorial. Journal of Cognition 2018;1:9. https://doi.org/10.5334/joc.10.
[58] Cohen J. Statistical Power Analysis for the Behavioral Sciences. 2nd ed. New York: Routledge; 1988. https://doi.org/10.4324/9780203771587.
[59] Wischnewski M, Schutter DJLG, Nitsche MA. Effects of beta-tACS on corticospinal excitability: A meta-analysis. Brain Stimulation 2019;12:1381–9. https://doi.org/10.1016/j.brs.2019.07.023.
[60] Bastani A, Jaberzadeh S. Differential modulation of corticospinal excitability by different current densities of anodal transcranial direct current stimulation. PLoS ONE 2013;8:e72254. https://doi.org/10.1371/journal.pone.0072254.
[61] Peterchev AV, Riehl ME. Transcranial Magnetic Stimulators. In: Wassermann EM, Peterchev AV, Ziemann U, Lisanby SH, Siebner HR, Walsh V, editors. The Oxford Handbook of Transcranial Stimulation, Oxford University Press; n.d., p. 0. https://doi.org/10.1093/oxfordhb/9780198832256.013.3.
[62] Aberra AS, Wang B, Grill WM, Peterchev AV. Simulation of transcranial magnetic stimulation in head model with morphologically-realistic cortical neurons. Brain Stimulation 2020;13:175–89. https://doi.org/10.1016/j.brs.2019.10.002.
[63] Aberra AS, Peterchev AV, Grill WM. Biophysically realistic neuron models for simulation of cortical stimulation. J Neural Eng 2018;15:066023. https://doi.org/10.1088/1741-2552/aadbb1.
[64] Barker AT, Garnham CW, Freeston IL. Magnetic nerve stimulation: the effect of waveform on efficiency, determination of neural membrane time constants and the measurement of stimulator output. Electroencephalogr Clin Neurophysiol Suppl 1991;43:227–37.

[65] Nowak LG, Bullier J. Axons, but not cell bodies, are activated by electrical stimulation in cortical gray matter. II. Evidence from selective inactivation of cell bodies and axon initial segments. Exp Brain Res 1998;118:489–500. https://doi.org/10.1007/s002210050305.
[66] Nowak LG, Bullier J. Axons, but not cell bodies, are activated by electrical stimulation in cortical gray matter. I. Evidence from chronaxie measurements. Exp Brain Res 1998;118:477–88. https://doi.org/10.1007/s002210050304.
[67] Di Lazzaro V, Oliviero A, Saturno E, Pilato F, Insola A, Mazzone P, et al. The effect on corticospinal volleys of reversing the direction of current induced in the motor cortex by transcranial magnetic stimulation. Exp Brain Res 2001;138:268–73. https://doi.org/10.1007/s002210100722.
[68] Di Lazzaro V, Rothwell JC. Corticospinal activity evoked and modulated by non-invasive stimulation of the intact human motor cortex. J Physiol 2014;592:4115–28. https://doi.org/10.1113/jphysiol.2014.274316.
[69] Biabani M, Aminitehrani M, Zoghi M, Farrell M, Egan G, Jaberzadeh S. The effects of transcranial direct current stimulation on short-interval intracortical inhibition and intracortical facilitation: a systematic review and meta-analysis. Rev Neurosci 2018;29:99–114. https://doi.org/10.1515/revneuro-2017-0023.
[70] Guerra A, Pogosyan A, Nowak M, Tan H, Ferreri F, Di Lazzaro V, et al. Phase Dependency of the Human Primary Motor Cortex and Cholinergic Inhibition Cancelation During Beta tACS. Cerebral Cortex 2016;26:3977–90. https://doi.org/10.1093/cercor/bhw245.
[71] Antal A, Paulus W. Transcranial alternating current stimulation (tACS). Front Hum Neurosci 2013;7. https://doi.org/10.3389/fnhum.2013.00317.
[72] Matsumoto H, Ugawa Y. Adverse events of tDCS and tACS: A review. Clin Neurophysiol Pract 2017;2:19–25. https://doi.org/10.1016/j.cnp.2016.12.003.
[73] Khanna P, Totten D, Novik L, Roberts J, Morecraft RJ, Ganguly K. Low-frequency stimulation enhances ensemble co-firing and dexterity after stroke. Cell 2021;184:912-930.e20. https://doi.org/10.1016/j.cell.2021.01.023.
[74] Hallez H, Vanrumste B, Grech R, Muscat J, De Clercq W, Vergult A, et al. Review on solving the forward problem in EEG source analysis. Journal of NeuroEngineering and Rehabilitation 2007;4:46. https://doi.org/10.1186/1743-0003-4-46.
[75] Ghafoor U, Yang D, Hong K-S. Neuromodulatory Effects of HD-tACS/tDCS on the Prefrontal Cortex: A Resting-State fNIRS-EEG Study. IEEE J Biomed Health Inform 2022;26:2192–203. https://doi.org/10.1109/JBHI.2021.3127080.
[76] Herrmann CS, Strüber D, Helfrich RF, Engel AK. EEG oscillations: From correlation to causality. Int J Psychophysiol 2016;103:12–21. https://doi.org/10.1016/j.ijpsycho.2015.02.003.
[77] Fehér KD, Morishima Y. Concurrent Electroencephalography Recording During Transcranial Alternating Current Stimulation (tACS). J Vis Exp 2016:e53527. https://doi.org/10.3791/53527.
[78] Di Gregorio F, Trajkovic J, Roperti C, Marcantoni E, Di Luzio P, Avenanti A, et al. Tuning alpha rhythms to shape conscious visual perception. Curr Biol 2022;32:988-998.e6. https://doi.org/10.1016/j.cub.2022.01.003.
[79] Kasten FH, Negahbani E, Fröhlich F, Herrmann CS. Non-linear transfer characteristics of stimulation and recording hardware account for spurious low-frequency artifacts during amplitude modulated transcranial alternating current stimulation (AM-tACS). Neuroimage 2018;179:134–43. https://doi.org/10.1016/j.neuroimage.2018.05.068.